

Pyrrolosporin A, a New Antitumor Antibiotic from *Micromonospora* sp. C39217-R109-7**II. Isolation, Physico-chemical Properties, Spectroscopic Study and X-ray Analysis**

DANIEL R. SCHROEDER*, KIMBERLY L. COLSON, STEVE E. KLOHR,
MIKE S. LEE and JAMES A. MATSON

Bristol-Myers Squibb Pharmaceutical Research Institute,
5 Research Parkway, P.O. Box 5100, Wallingford, Connecticut 06492, U.S.A.

LINDA S. BRINEN and JON CLARDY

Department of Chemistry, Baker Laboratory, Cornell University,
Ithaca, New York 14853, U.S.A.

(Received for publication March 6, 1996)

Pyrrolosporin A (**1**) is a new macrolide antitumor antibiotic possessing an unusual spiro- α -acyltetronic acid moiety. The antibiotic was isolated from the fermentation broth of *Micromonospora* sp. by vacuum liquid chromatography, crystallization and reversed phase HPLC (C18). The structure was determined by a combination of NMR, MS, IR, UV, X-ray analysis and degradation studies.

In the course of screening for new antitumor antibiotics, a new metabolite of *Micromonospora* sp. (ATCC 53791) was discovered and evaluated¹) as a potential development candidate. In this paper we present the isolation, physico-chemical properties, degradation studies and structure determination, including complete NMR assignments and an X-ray analysis.

Isolation

The fermentation of pyrrolosporin A was carried out as described in the preceding article²). Whole broth was extracted successively with ethyl acetate, and the combined organic layers concentrated under reduced pressure. Initially, the isolation of pyrrolosporin A was accomplished using solvent partitioning, size exclusion chromatography (Sephadex LH-20) and reversed phase HPLC (C18). The activity was monitored by cytotoxicity (HCT 116, human colon tumor) and antibacterial screening (Gram-positive bacteria). The presence of the pyrrolosporin A in chromatographic fractions was easily determined by silica gel TLC using short-wavelength UV light and vanillin spray reagent (0.5% vanillin in H₂SO₄ - ethanol 4:1, with heating). Under these conditions pyrrolosporin A turns an intense blue color. The structure for pyrrolosporin A (**1**) is shown in Fig. 1.

Subsequently larger quantities of pyrrolosporin A were required for biological evaluation and a process amenable to scale up was developed (Fig. 2). Successive vacuum liquid chromatography (VLC) step gradients on crude

extract resulted in a large mass reduction. Solids were preadsorbed onto silica gel (Lichroprep Si 60, 25~40 microns, E. Merck) and predetermined volumes of hexane, containing increasing amounts of acetone or ethyl acetate, were pulled through the silica gel bed and concentrated. The advanced fraction (13 g) from these adsorption chromatographies was dissolved in 100 ml of hot acetonitrile. Before substantial cooling had even occurred, the pyrrolosporin complex crystallized out from the remaining unrelated impurities. Final purification of the major component, pyrrolosporin A, was accomplished with reversed phase HPLC (C18) using

Fig. 1. Structure of pyrrolosporin A (**1**).

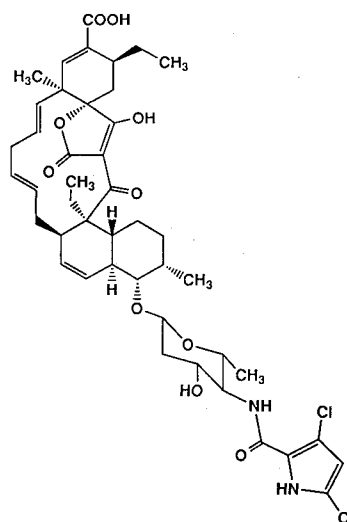


Fig. 2. Isolation process for pyrrolosporin A.

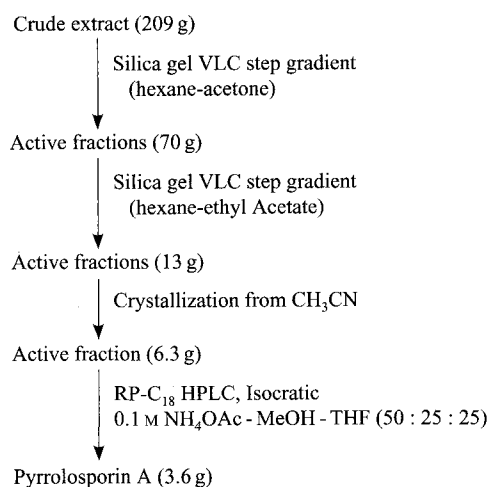


Table 1. Physico-chemical properties of pyrrolosporin A.

Appearance	White crystalline solid
MP	235°C
$[\alpha]_D^{26}$	+2.8 (<i>c</i> , 0.2 in methanol)
Molecular formula	$C_{44}H_{54}Cl_2N_2O_{10}$
FAB-MS (<i>m/z</i>) neg. ion (NBA)	839 ($M-H$) ⁻
HRFAB-MS (<i>m/z</i>)	
Obs.	879.2783 ($M+K$) ⁺
Calcd	879.2793
	for $C_{44}H_{54}Cl_2N_2O_{10}K$
UV λ_{max} nm (ϵ)	268 (341), methanol
TLC (Rf), Merck silica gel 60, F ₂₅₄ , Art. 5917	0.30, Chloroform - methanol 90 : 10
HPLC (Rt), Rainin C18 microorb-MV column, 4.6 × 150 mm, 5 micron	Retention time 6.7 minutes, isocratic, 1.2 ml/minute, CH ₃ CN - H ₂ O 70 : 30, 10 mM phosphate buffer, pH 3.5
pKa's	
pKa(1)	2.95
pKa(2)	5.39

isocratic conditions (0.1 M NH₄OAc - MeOH - THF 50 : 25 : 25).

Physico-chemical Properties

Pyrrolosporin A was isolated as a white crystalline solid. It is soluble in most organic solvents including chloroform, ethyl acetate, acetone, methanol, pyridine, tetrahydrofuran, and dimethyl sulfoxide, but insoluble in hexanes, toluene, acetonitrile and water. Additional physico-chemical properties for pyrrolosporin A are provided in Table 1. It is a weakly dextrorotatory compound. Determination of the pKa's was made in a 20% aqueous-methanol solution due to the insolubility of pyrrolosporin A in water. The titration was performed

Fig. 3. IR (film) spectrum for pyrrolosporin A.

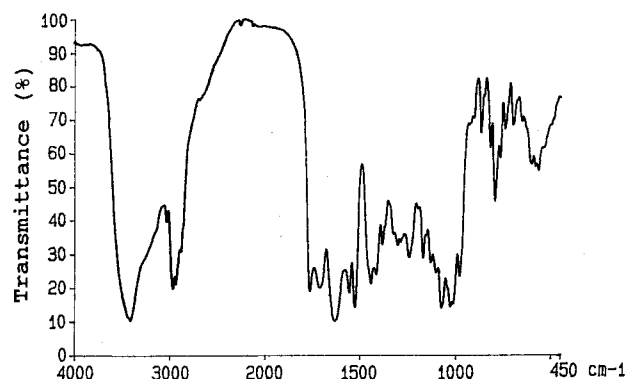
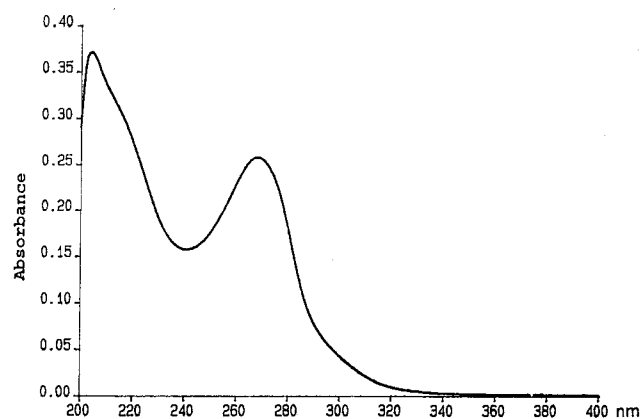


Fig. 4. UV spectrum for pyrrolosporin A (MeOH).



with dilute NaOH. Citric and benzoic acid standards, for which the aqueous pKa's are known, were analyzed in the same manner. A linear relationship was evident from a plot of the combined data, from which the aqueous pKa's for pyrrolosporin A were calculated. The IR and UV spectra for pyrrolosporin A are shown in Fig. 3 and Fig. 4, respectively. A molecular weight of 840 corresponds to the molecular formula $C_{44}H_{54}Cl_2N_2O_{10}$ as determined by HR-FAB-MS.

Acidic Methanolysis of Pyrrolosporin A

Pyrrolosporin A was allowed to stir in anhydrous methanol containing 0.5 N HCl at room temperature for 5 days. At the end of this time no starting material remained, and three new UV quenching zones were visible by TLC. After purification on silica gel, the aglycone of pyrrolosporin A, now named pyrrolosporide (2), was obtained as a major product, MW 550, $C_{33}H_{42}O_7$; HR-FAB-MS ($M+Na$)⁺ *m/z* 573.2806, calcd 573.2828 (Fig. 5). The methyl ester of pyrrolosporide (3) was isolated as a minor product; MW 564 corresponding to

$C_{34}H_{44}O_7$; HR-FAB-MS $(M+H)^+$ m/z 565.3158, calcd 565.3165. The antibiotic sugar was obtained as the α -methyl glycoside (**4**), still possessing the chlorinated pyrrole *via* the amide linkage. Compound **4** was also a major product, MW 322, indicating $C_{12}H_{16}Cl_2N_2O_4$ as

the molecular formula; HR-FAB-MS $(M+Na)^+$ m/z 345.0386, calcd 345.0385.

NMR Analysis

The ^{13}C NMR spectrum for pyrrolosporin A (**1**) showed significant line broadening of resonances centered around the tetronic acid moiety, to the extent that several resonances appeared to be absent. This was also the case with the aglycone (**2**). Presumably this was due to tautomerism³⁾, and upon addition of a small amount of DCl, the signals sharpened up. The 1H NMR and ^{13}C NMR spectra for pyrrolosporin A are presented in Figs. 6 and 7, respectively. Complete chemical shift assignments are presented in Table 2. The carbon count for pyrrolosporin A was established at 44 carbons using the fully decoupled, inverse gated ^{13}C NMR experiment, for which the resonances are integratable. The DEPT

Fig. 5. Methanolysis products of pyrrolosporin A.

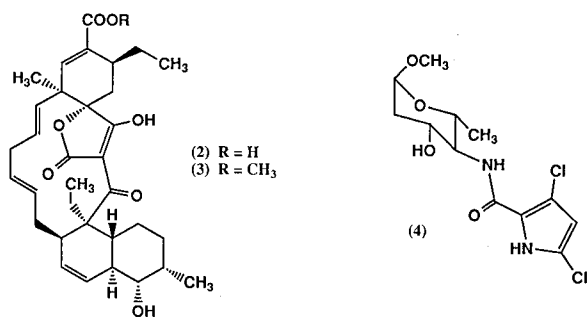


Fig. 6. 1H NMR spectrum for pyrrolosporin A (500 MHz, d_6 -DMSO).

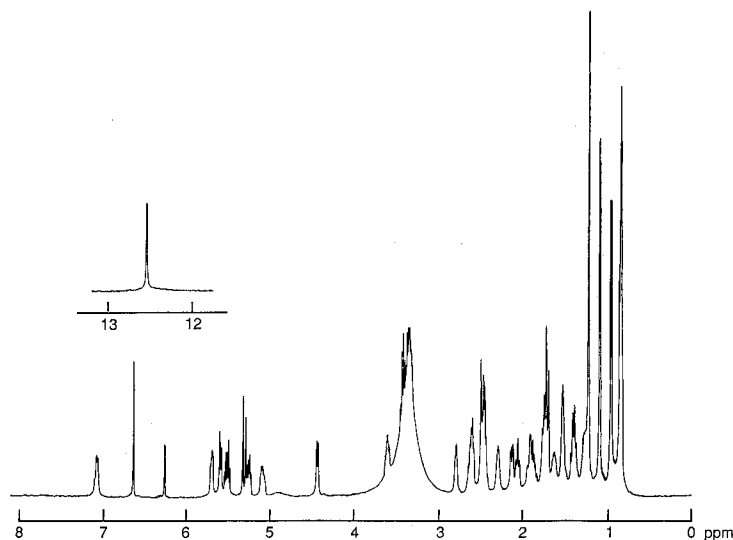


Fig. 7. ^{13}C NMR spectrum for pyrrolosporin A (125 MHz, d_6 -DMSO).

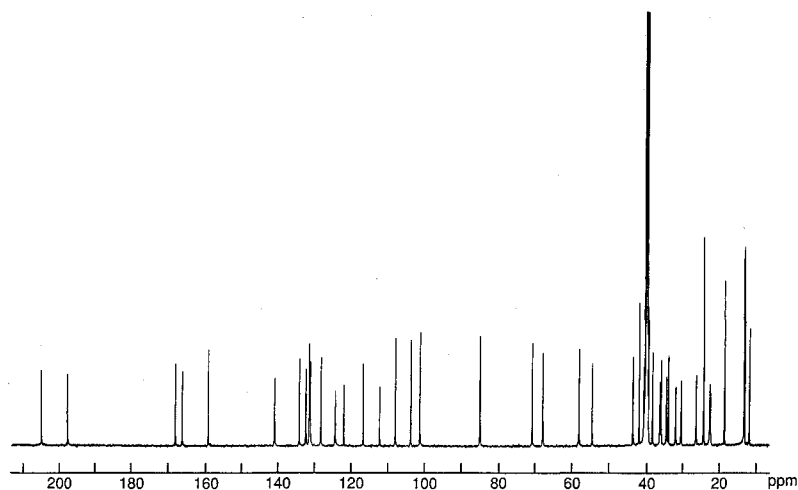
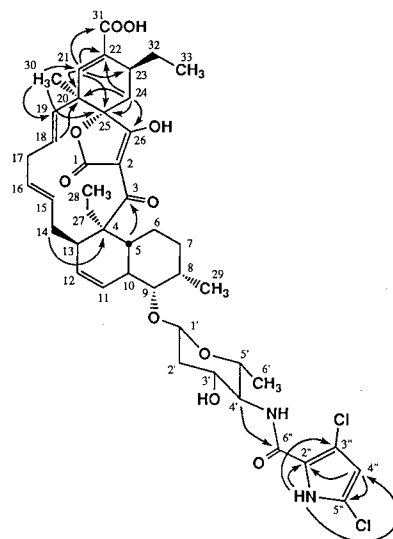


Table 2. Pyrrolosporin A (1): ^1H and ^{13}C NMR Assignments (d_6 -DMSO).

Carbon	^{13}C ppm (mult)	^1H ppm [mult, J (Hz) ^a]
Macrocycle		
1	165.9 (s)	
2	103.8 (s)	
3	204.9 (s)	
4	54.4 (s)	
5	39.6 (d)	1.73 (m)
6	22.2 (t)	Ha 1.70 (m) Hb 1.25 (m)
7	31.7 (t)	Ha 1.49 (m) Hb 1.49 (m)
8	33.7 (d)	2.28 (m, 6.63)
9	84.9 (d)	3.30 (dd, 10.3, 2.9)
10	38.0 (d)	2.05 (ddd, 10.3, 10.2, 9.5)
11	124.3 (d)	5.59 (br dd, 17.5, 7.5, 2.9)
12	131.2 (d)	5.67 (dd, 10.2, 7.4)
13	43.3 (d)	2.77 (dd, 7.9, 7.4)
14	36.0 (t)	Ha 1.91 (m, 8.4) Hb 1.86 (m, 7.9)
15	131.4 (d)	5.07 (dd, 14.8, 8.4)
16	128.2 (d)	5.24 (d, 14.8)
17	34.2 (t)	Ha 2.49 (m) Hb 2.49 (m)
18	131.1 (d)	5.51 (d, 15.8)
19	132.3 (d)	5.29 (d, 15.8)
20	41.6 (s)	
21	140.8 (d)	6.63 (s)
22	134.1 (s)	
23	35.6 (d)	2.60 (d, 7.4)
24	30.2 (t)	Ha 2.50 (m) Hb 1.72 (m)
25	85.0 (s)	
26	197.5 (s)	
27	22.4 (t)	Ha 2.60 (dd, 12.7, 5.5) Hb 1.77 (dd, 12.7, 10.9)
28	12.9 (q)	0.84 (s)
29	13.2 (q)	0.94 (d, 6.63)
30	24.1 (q)	1.22 (s)
31	167.8 (s)	
32	26.1 (t)	Ha 1.68 (br dd, 17.5, 7.5, 2.9) Hb 1.40 (br dd, 17.5, 4.3, 2.9)
33	11.6 (q)	0.82 (s)
Amino sugar		
1'	101.3 (d)	4.42 (d, 9.4)
2'	40.3 (t)	eq 2.13 (dd, 12.1, 4.9) ax 1.40 (ddd, 12.1, 11.1, 9.4)
3'	67.9 (d)	3.61 (ddd, 11.1, 8.9, 4.9)
4'	58.0 (d)	3.43 (ddd, 9.7, 8.9, 8.2)
5'	70.7 (d)	3.34 (dd, 9.7, 6.0)
6'	18.4 (q)	1.08 (d, 6.0)
3'-OH		Exchanged
4'-NH		7.01 (d, 8.2)
Pyrrolamide ^b		
1''-NH		12.52 (d, 2.2)
2''	122.8 (s)	
3''	112.3 (s)	
4''	108.0 (d)	6.21 (d, 2.2)
5''	116.8 (s)	
6''	158.9 (s)	

^a Due to overlapping resonances, several proton coupling constants were not obtainable, and some were gleaned while conducting single irradiation decoupling experiments.

^b Because 2-bond and 3-bond carbon-proton coupling constants for pyrroles are of the same magnitude, it was not possible to prove all assignments of carbon resonances using 2D NMR (COLOC and HMBC) experiments, so chemical shift arguments and comparisons with known chlorinated pyrroles were utilized.

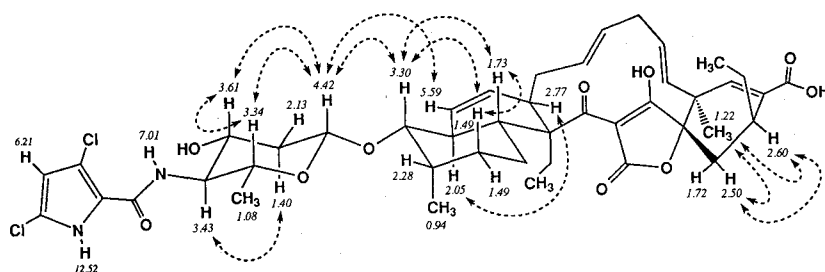
Fig. 8. Selected long-range ^1H - ^{13}C heteronuclear correlations for pyrrolosporin A that tie in quaternary carbons.

and HETCOR experiments indicated 13 quaternary, 18 methine, 8 methylene and 5 methyl carbons. The proton NMR revealed 49 protons directly bonded to carbons, leaving 5 exchangeable protons as follows: 1 amide NH, 1 carboxylic acid, 1 hydroxyl, 1 pyrrole NH and 1 tetrone acid OH. The connectivity was established through a series of 1D and 2D NMR experiments including the COLOC, HMBC, and COSY experiments. Selected long range ^1H - ^{13}C heteronuclear data is presented in Fig. 8.

The spiro- α -acyltetrone moiety consists of 5 quaternary carbons, 4 oxygens, and one exchangeable proton. These atoms are further linked to quaternary carbons on either end (C4 and C20). A large three bond heteronuclear coupling (9.6 Hz) between H-5 and C3 established the C4 linkage to the octalin rings (Fig. 8), and several long range correlations were observed from nearby protons to the C20, C25 and C26 quaternary carbons, but no coherences were observed to the C1 and C2 carbons, which are singlets in the fully coupled ^{13}C NMR spectrum.

The cyclohexene ring was defined mainly by the COLOC and HMBC experiments. The carboxyl group could be placed on C22 by a coherence between the vinyl proton H-21, and C31 (6.3 Hz). Several other key long-range coherences were revealed from the H-21 methine, as well as the H-24 methylene and H-30 methyl, to quaternary carbons (Fig. 8). The cyclohexene ring appears to be in a half-boat conformation in solution, with the ethyl group axial to avoid eclipsing the carboxyl group on C22. An observed NOE (Fig. 9) between the

Fig. 9. Selected nOe data for pyrrolosporin A from single irradiation experiments.



H-30 methyl, which is also positioned axial, and the H-23 methine established the relative stereochemistry between the C20 and C23 centers, but it was not possible by NMR to prove the stereochemistry of the spiro center C25, relative to the adjacent quaternary C20, or relative to the stereocenters on the lower portion of the molecule (e.g., C4 and C13).

The 15 consecutive proton bearing carbons from C5 to C19 constitute one large proton spin system. This segment of the structure was readily assembled using 2D-COSY data in conjunction with information obtained from 1D decoupling experiments. The trans ring fusion of the octaline rings (H-5 to H-10, $J=9.5$ Hz) and the diaxial relationship between H-10 and H-9 ($J=10.3$ Hz) was evident from ^1H - ^1H coupling constant information as was the syn relationship between H-9 and H-8 ($J=2.9$ Hz). Only a limited amount of additional structural information was obtained from the NOE analysis, but interactions were observed between H-5 and H-9, H-5 and H $_{\beta}$ -7, and H-9 and H $_{\beta}$ -7 which are all positioned axial on the same face of the ring (Fig. 9). These adjacent trans fused rings are clearly in boat, and half-boat conformations, as was the case with kijanimicin and the rest of the members of the class.

The three bond coherence between H-1' and C-9, that would have placed the sugar side chain on the aglycone, was not observed in the HMBC or COLOC experiments. The linkage was supported by NOE interactions between H-1' and both H-9 and H-11 (Fig. 9). The coupling constant for the anomeric proton (9.4 Hz) clearly indicated a β linkage for the sugar. Strong NOE's between the protons H-1', H-3' and H-5', and between H-2' $_{ax}$ and H-4' confirmed a chair conformation with equatorial substituents. In agreement, ^1H - ^1H coupling constants indicated the successive diaxial relationship between protons starting at H-1', and continuing around the ring to H-5'. Connectivity of the pyrrole to the sugar *via* an amide linkage was supported by long-range correlations from both H-4', and the adjacent NH, to C6'' (Fig. 8).

The COSY spectrum revealed a "W" planar, 4-bond ^1H - ^1H coupling (2.2 Hz) between the pyrrole NH (12.52 ppm) and H-4'' (6.21 ppm). Both of these protons showed both two and three bond long-range correlations to quaternary carbons in the pyrrole ring as depicted in Fig. 8.

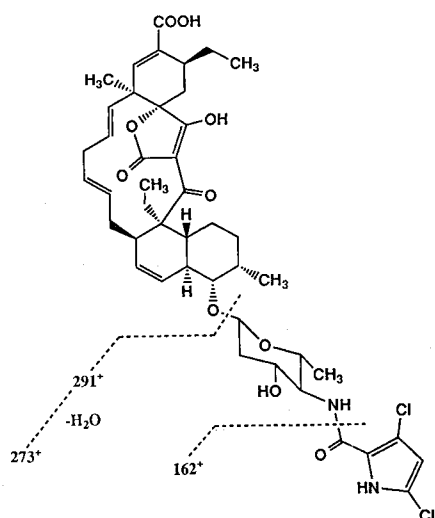
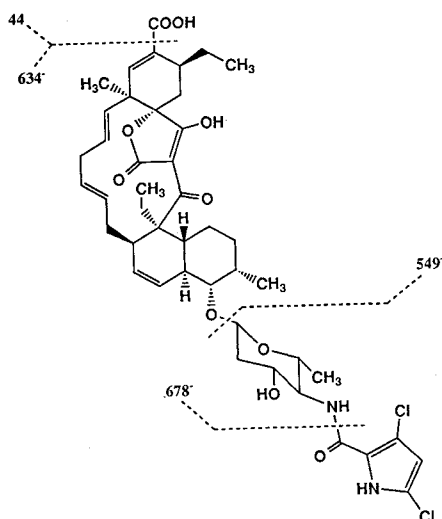
MS Analysis

The full scan FAB mass spectra of pyrrolosporin A indicated the molecular weight to be 840. The positive ion FAB-MS analysis showed intense potassium adduct ions for $[\text{M} + \text{K}]^+$, $[\text{M} + 2\text{K} - \text{H}]^+$ and $[\text{M} + 3\text{K} - 2\text{H}]^+$ at m/z 879, 917 and 955, respectively (NBA/AcOH/KI matrix). The negative ion FAB mass spectrum contained an abundant deprotonated molecular ion $[\text{M} - \text{H}]^-$ at m/z 839. A close inspection of the isotopic abundances of the molecular ion clusters indicated that pyrrolosporin A contained two atoms of chlorine. The high resolution FAB-MS measurement carried out on the potassium adduct ion $[\text{M} + \text{K}]^+$ at m/z 879 indicated a molecular formula of $\text{C}_{44}\text{H}_{54}\text{Cl}_2\text{N}_2\text{O}_{10}\text{K}$.

Further analysis of the positive ion FAB mass spectrum (Fig. 10) revealed prominent ions at m/z 291 consistent with the entire sugar side chain, as well as a m/z 162 ion indicating the terminal carbonyl-pyrrole portion only. The isotopic ratio indicated that both of these ions were dichlorinated.

Negative ion FAB-MS-MS yielded complementary information as product ions corresponding to the aglycone portion rather than the sugar side chain were observed (Fig. 11). The deprotonated molecular ion at m/z 839 yielded product ions at m/z 678 and m/z 549. Close inspection of the full scan FAB mass spectrum revealed that these ions were not chlorinated. HRFAB-MS analysis determined the accurate mass of the fragment ion to be 678.3613, corresponding to a molecular formula of $\text{C}_{39}\text{H}_{52}\text{NO}_9$. This resulted from the neutral loss (-161) of the terminal carbonyl-pyrrole moiety. A further neutral loss (-147) of the sugar moiety

Fig. 10. Positive ion FAB-MS data for pyrrolosporin A.

Fig. 11. Negative ion FAB-MS-MS data for pyrrolosporin A; daughter ions of m/z 839⁻.

yielded a rather unusual fragment ion (probably an elimination process resulting in a double bond at C9–C10) with an accurate mass of 531.2745 ($C_{33}H_{39}O_6$). The 531 ion was actually substantially more abundant than the 549 ion, and misled us regarding the structure of the sidechain in the early studies of pyrrolosporin A. Substructure analysis involving the m/z 678 ion also revealed an abundant fragment ion at m/z 634 corresponding to a further loss of 44 amu and suggested a carboxylic acid moiety.

X-ray Analysis of Pyrrolosporin

In order to confirm the stereochemical assignments made by NMR as well as to elucidate the stereochemistry of C25 relative to C20 and the lower portion of the

Fig. 12. X-ray structure of pyrrolosporin A.

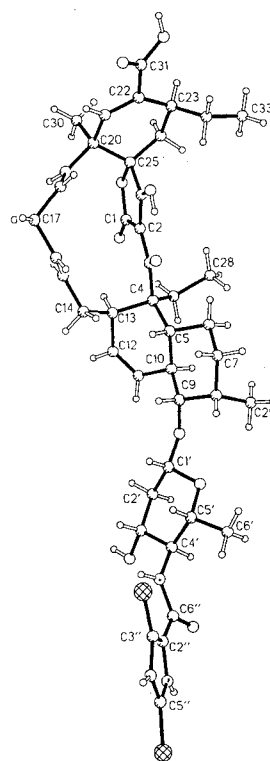


Table 3. Single crystal X-ray crystallographic analysis.

Crystal parameters	
Empirical formula	$C_{44}H_{54}N_2Cl_2O_{10} \cdot (CH_3CN)_2$
Formula weight	841.8
Crystal dimensions (mm)	$0.05 \times 0.2 \times 0.4$
Crystal system	Monoclinic
Lattice parameters	$a = 32.474(11) \text{ \AA}$ $b = 9.301(4) \text{ \AA}$ $c = 15.603(8) \text{ \AA}$ $\beta = 90.39(1)^\circ$
Space group	$C2$ with $Z = 2$
Density (g/cm^3)	1.19
Linear absorption factor (cm^{-1})	16.86
Refinement parameters	
No. of reflections measured	3445
Observed reflections ($I > 2\sigma$)	2676
R-index (R, Rw)	6.23%, 7.77%
Goodness of fit parameter	1.83

molecule, a single crystal X-ray crystallographic analysis of pyrrolosporin A was undertaken on a sample crystallized from acetonitrile. The relative configuration obtained is shown in Fig. 12. The structure was solved by direct methods and the non-hydrogen atoms were refined anisotropically. The final agreement factor, R, is

0.0623. A flat rectangular plate with approximate dimensions $0.05 \times 0.2 \times 0.4$ mm was used on a Siemens P3 diffractometer with graphite monochromated $\text{CuK}\alpha$ radiation. Data were collected at ambient temperature using $\nu:2\nu$ scans to a maximum 2ν of 115.0° . Pertinent crystal data are summarized in Table 3.

Discussion

With the exception of the spiro- α -acyltetronic acid moiety, the connectivity for pyrrolosporin A was readily established using 2D NMR techniques. The presence of the tetronic acid ring could only be inferred based on chemical shift arguments, the unsaturation number, and other physio-chemical data. The unsaturation number, 18, derived from the molecular formula, indicated 7 rings after the 5 carbonyls and 6 double bonds were taken into account. It required the X-ray analysis to establish the complete relative stereochemistry for the molecule, as well as to prove the substitution pattern on the dichlorinated pyrrole ring. The absolute stereochemistry for pyrrolosporin A has not been established.

Pyrrolosporin A is a new member of a small class of condensed macrolactones with a 13-membered macrolide ring. It incorporates parts of cyclohexene and octalin ring systems, with a spiro- α -acyltetronic acid moiety to form an interesting macrocyclic structure. Only two complexes of antibiotics having identical ring systems in the aglycone portion have been reported previously, namely, the kijanimicins⁴⁾ and the tetrocarcins⁵⁾, both antitumor antibiotics. In addition, there are several other compounds which are very closely related that incorporate an additional oxygen into the macrocyclic ring forming 14-membered ring lactones. Examples of this type are the chlorothricins^{6,7)} and the PA-46101 complex⁸⁾. It is worth noting that the stereochemistry at C20, for attachment of the aliphatic portion to the cyclohexene ring, is opposite to what was previously observed for the rest of the members of the class. This results in a different orientation of the cyclohexene ring relative to the distant octalin rings as compared to kijanimicin and the tetrocarcin.

Although pyrrolosporin A has many structural features in common with the related compounds above, the chlorinated pyrrole is a novel feature. Also the 4-amino-2,4,6-trideoxy- β -D-arabino-hexopyranosyl moiety, now designated as pyrrolosamine, has not been documented in the literature as a naturally occurring sugar, but one recent account of a synthesis⁹⁾ was found. Low molecular weight chlorinated pyrroles such as the pyrrolomycins¹⁰⁾ and pyoluteorin¹¹⁾ have been reported in the literature which show antibacterial and antifungal properties.

Experimental

Two quite different isolation processes are presented below; a laboratory scale isolation on residues from a

shake flask culture (the actual discovery of pyrrolosporin A), and a preparative scale isolation on extract obtained from a pilot plant fermenter.

Laboratory Scale Isolation of Pyrrolosporin A

Whole fermentation broth (10 liters) from a shake flask culture²⁾ was extracted with ethyl acetate (4 liters). The ethyl acetate layer yielded 630 mg of crude extract upon evaporation under reduced pressure.

A portion of the crude extract (220 mg) was purified by solvent partitioning. The residue was dissolved in 10% aqueous methanol (100 ml) and partitioned against hexanes (100 ml, presaturated with 10% aqueous methanol) in a 500 ml separatory funnel. The layers were separated and the aqueous methanol layer (bottom) was washed an additional two times with fresh hexanes. The combined hexane layers were concentrated to yield 49 mg residue.

Water (20 ml) was added to the aqueous methanol layer to yield 120 ml of 25% aqueous methanol. This layer was further partitioned against 120 ml of carbon tetrachloride (presaturated with 25% aqueous methanol) and the layers separated. Two additional washes of the aqueous methanol with carbon tetrachloride yielded 43 mg residue upon concentration of the combined organic layers.

More water (20 ml) was added to the aqueous methanol to yield 140 ml of 35% aqueous methanol. This was partitioned against 140 ml of chloroform (presaturated with 35% aqueous methanol) and the layers separated. The bottom layer, when combined with two additional chloroform washes (as above) yielded 86 mg residue upon removal of solvent under reduced pressure.

Evaporation of the residual 35% aqueous methanol layer resulted in a fourth residue (25 mg).

The carbon tetrachloride and chloroform residues (125 mg) from the Kupchan distribution experiment were combined in 2 ml of chloroform-methanol (1:1) and applied to a Glenco column (i.d. 2.5 cm \times 100 cm) containing 140 g of Sephadex LH-20 preswollen in chloroform-methanol (1:1). A flow rate of 1.5 ml/minute was maintained. After a 90 ml void volume, twenty 15 ml tubes were collected, followed by a 500 ml wash volume of the same eluant. TLC analysis indicated a major UV quenching zone (254 nm) in tubes 9~11 (one-half bed volume) which gave a blue color with vanillin spray reagent and heating (see Table 1 and Isolation section). These tubes were combined and concentrated to yield 52 mg of residue.

The 52 mg residue from the sizing column was dissolved in 0.5 ml DMSO and injected onto a Whatman RP-C18 column (Partisil 10, ODS-3, i.d. 10 mm \times 50 cm) equilibrated with 0.1 M ammonium acetate-methanol-tetrahydrofuran (50:25:25)—isocratic; flow rate 4 ml/minute; detection at 254 nm. The material of interest eluted in 20.5 minutes over two fractions. These fractions were pooled, extracted with two 25 ml volumes of chloroform, and the combined organic layers con-

centrated to dryness to yield pyrrolosporin A (16.7 mg) as a white solid.

Preparative Scale Isolation of Pyrrolosporin A

A portion (209 g) of a 1.72 kg crude ethyl acetate extract resulting from a 680 liter pilot plant fermentation²⁾ was redissolved in ethyl acetate and adsorbed onto 300 g Universal silica gel 60 (Woelm, 63~200 microns). This material was applied as a hexane slurry to a 3 liter sintered glass funnel (Kontes, M porosity, 15 cm i.d.) containing an additional 900 g silica gel pre-equilibrated with hexanes. A step gradient was carried out by sucking successive 3 liter volumes of hexanes with increasing amounts of acetone (containing 1% glacial acetic acid) through the silica gel bed into a large Erlenmeyer vacuum flask. In this manner nine fractions were generated which were concentrated under reduced pressure. Residual acetic acid was removed azeotropically with cyclohexane. The amount of acetone contained in the mobile phase of the first 8 fractions was 5%, 10%, 20%, 30%, 30%, 40%, 60%, 100%, followed by a ninth fraction consisting of ethyl acetate-methanol 2:1. On the basis of TLC analysis, fraction 6 had the highest concentration of pyrrolosporin A, with lesser amounts in fractions 5 and 7. The combined fractions 5~7 weighed 70 g. The anti-foam used in the fermentation tanks, polypropylene glycol (ppg), elutes on silica gel with hexane-30% acetone, thus fraction 4 had the bulk of the anti-foam, trailing into fraction 5.

The advanced fraction (70 g) was again dissolved in ethyl acetate and adsorbed onto 150 g Universal silica gel 60 (Woelm, 63~200 microns). This material was applied as a hexane slurry to a somewhat smaller, 2 liter sintered glass funnel (Kontes, M porosity, 13 cm i.d.) containing an additional 650 g silica gel pre-equilibrated with hexanes. Again a step gradient was carried out by sucking 3 liter volumes of hexanes, but this time with increasing amounts of ethyl acetate, through the silica gel bed into a vacuum flask. No glacial acetic acid was used in this experiment (but in retrospect should have been used, because it prevents band tailing which is a problem with pyrrolosporin A, which possesses a free carboxylic acid moiety). Six fractions were collected which were combined on the basis of TLC analysis, and concentrated under reduced pressure. The amount of ethyl acetate contained in the mobile phase for the six fractions was 40%, 50%, 50%, 50%, 50%, and 100%. Pyrrolosporin A was spread over fractions 2~5, the highest concentration being in fraction 2 (6 g).

The combined VLC fractions 2~5 (13 g) were placed in a Erlenmeyer flask (500 ml) with 100 ml of acetonitrile and heated on a steam bath. At the boiling point the solids dissolved completely and began crystallizing out before substantial cooling had occurred. The crystalline precipitate (6.3 g) was collected by vacuum filtration on a Buchner funnel. In this manner, unrelated impurities were removed from the pyrrolosporin complex.

Reversed phase HPLC (C18) was the final purification

step used to achieve homogeneity of the major component, pyrrolosporin A. DMSO solutions (200 mg/ml) of the crystalline precipitate, were injected (0.5 ml) onto a Rainin Dynamax-60A column equipped with a guard module (RP-C18, 8 micron, i.d. 21.4 mm x 30 cm), flow rate 20 ml/minute, detection at 254 nm, using isocratic conditions (0.1 M ammonium acetate-methanol-tetrahydrofuran 50:25:25). The combined eluant from successive runs of the major peak (Rt 23 minutes) was concentrated to a small aqueous volume on a rotary evaporator and extracted twice with chloroform, dried with brine, and concentrated. In this manner 3.6 g of pyrrolosporin A was obtained from 209 g crude extract.

Acknowledgments

The authors thank K. S. LAM and D. R. GUSTAVSON for fermentation support, and D. BUTCHER for analytical services.

References

- SCHROEDER, D. R.; K. S. LAM, G. A. HESLER, D. R. GUSTAVSON, K. TOMITA & R. L. BERRY: Antitumor antibiotic BMY-42448. U.S. Patent No. 5,082,933 issued January 21, 1992. Pyrrolosporin A was previously referred to as BMY-42448
- LAM, K. S.; G. A. HESLER, D. R. GUSTAVSON, R. L. BERRY, K. TOMITA, J. L. MACBETH & S. FORENZA: Pyrrolosporin A, a new antitumor antibiotic from *Micromonospora* sp. C39217-R109-7. I. Taxonomy of the producing organism, fermentation and biological activity. *J. Antibiotics* 49: 860~864, 1996
- GELIN, S. & P. POLLET: Tautomerism in acyl tetronic acids. *Tetrahedron Lett.* 21: 4491~4494, 1980
- MALLAMS, A. K.; M. S. PUAR & R. R. ROSSMAN: Kijanamicin. Part 3. Structure and absolute stereochemistry of kijanamicin. *J. Chem. Soc. Perkin Trans. I* 1983: 1497~1534, 1983
- HIRAYAMA, N.; M. KASAI, K. SHIRAHATO, Y. OHASHI & Y. SASADA: The structure of tetronolide, the aglycone of antitumor antibiotic tetrocarcin. *Tetrahedron Lett.* 21: 2559~2560, 1980
- MUNTWYLER, R. & W. KELLER-SCHLEIRLEIN: Die Struktur des Chlorothricins, eines neuartigen Makrolid-Antibiotikums. *Helv. Chim. Acta* 55: 2071~2094, 1972
- BRUFANI, M.; S. CERRINI, W. FEDELI, F. MAZZA & R. MUNTWYLER: Kristallstrukturanalyse des Chlorothricolid-methylesters. *Helv. Chim. Acta* 55: 2094~2102, 1972
- MATSUMOTO, M.; Y. KAWAMURA, Y. YOSHIMURA, Y. TERUI, H. NAKAI, T. YOSHIDA & J. SHOJI: Isolation, characterization and structures of PA-46101 A and B. *J. Antibiotics* 43: 739~747, 1990
- SHIBATA, Y.; Y. KOSUGE & S. OGAWA: Synthesis and biological activities of methyl oligobiosaminide and some deoxy isomers thereof. *Carbohydr. Res.* 199: 37~54, 1990
- KOYAMA, M.; N. EZAKI, T. TSURUOKA & S. INOUE: Structural studies on pyrrolomycins C, D and E. *J. Antibiotics* 36: 1483~1489, 1983
- BIRCH, A. J.; P. HODGE, R. W. RICKARDS, R. TAKEDA & T. R. WATSON: The structure of pyoluteorin. *J. Chem. Soc.* 2641~2644, 1964